

MICROCOPY RESOLUTION TEST CHART
1010-10A

DTIC FILE COPY

12

AFGL-TR-87-0133

MEM RESOLUTION OF LINE SPECTRA

B.K. Yap

Yap Analytics, Inc.
594 Marrett Road
Lexington, MA 02173

AD-A182 860

The work reported herein was performed under subcontract to
Center for Space Engineering
Utah State University
Logan, UT 84322-4140

Scientific Report No. 23

23 March 1987

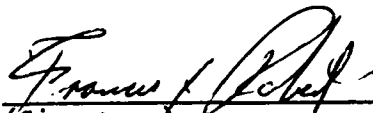
Approved for public release; distribution unlimited.

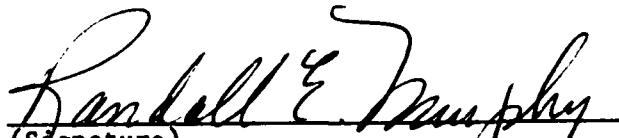
Prepared for:

AIR FORCE GEOPHYSICS LABORATORY
AIR FORCE SYSTEMS COMMAND
UNITED STATES AIR FORCE
HANSCOM AIR FORCE BASE, MA 01731

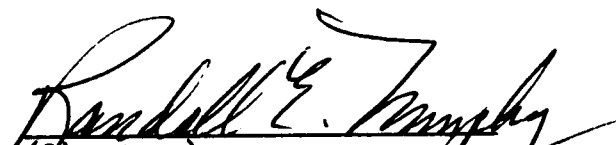
DTIC
ELECTE
JUL 22 1987
S
E
D

"This technical report has been reviewed and is approved for publication"


(Signature)
FRANCIS X. ROBERT
Contract Manager


(Signature)
RANDALL E. MURPHY, Acting Chief
Atmospheric Backgrounds Branch

FOR THE COMMANDER


(Signature)
RANDALL E. MURPHY, Director
Infrared Technology Division

This report has been reviewed by the ESD Public Affairs Office (PA) and is releasable to the National Technical Information Service (NTIS).

Qualified requestors may obtain additional copies from the Defense Technical Information Center. All others should apply to the National Technical Information Service.

If your address has changed, or if you wish to be removed from the mailing list, or if the addressee is no longer employed by your organization, please notify AFGL/DAA, Hanscom AFB, MA 01731. This will assist us in maintaining a current mailing list.

Do not return copies of this report unless contractual obligations or notices on a specific document requires that it be returned.

REPORT DOCUMENTATION PAGE

| | | | |
|---|--|--|---------------------------|
| 1a. REPORT SECURITY CLASSIFICATION Unclassified | | 1b. RESTRICTIVE MARKINGS None | |
| 2a. SECURITY CLASSIFICATION AUTHORITY | | 3. DISTRIBUTION/AVAILABILITY OF REPORT Approved for public release; distribution unlimited. | |
| 2b. DECLASSIFICATION/DOWNGRADING SCHEDULE N/A | | 4. PERFORMING ORGANIZATION REPORT NUMBER(S) CSE/87-011 | |
| 4. PERFORMING ORGANIZATION REPORT NUMBER(S) CSE/87-011 | | 5. MONITORING ORGANIZATION REPORT NUMBER(S) AFGL-TR-87-0133 | |
| 6a. NAME OF PERFORMING ORGANIZATION Center for Space Engineering Utah State University | 6b. OFFICE SYMBOL (If applicable) | 7a. NAME OF MONITORING ORGANIZATION Air Force Geophysics Laboratory | |
| 6c. ADDRESS (City, State and ZIP Code) Utah State University Logan, UT 84322-4140 | | 7b. ADDRESS (City, State and ZIP Code) Hanscom Air Force Base Bedford, MA 01731 | |
| 8a. NAME OF FUNDING/SPONSORING ORGANIZATION Air Force Geophysics Lab | 8b. OFFICE SYMBOL (If applicable) | 9. PROCUREMENT INSTRUMENT IDENTIFICATION NUMBER F19628-83-C-0056 | |
| 8c. ADDRESS (City, State and ZIP Code) Hanscom Air Force Base Bedford, MA 01731 | | 10. SOURCE OF FUNDING NOS. | |
| 11. TITLE (Include Security Classification) MEM Resolution of Line Spectra | | PROGRAM ELEMENT NO. 62101F | PROJECT NO. 7670 |
| 12. PERSONAL AUTHOR(S) B. K. Yap | | TASK NO. 10 | WORK UNIT NO. AK |
| 13a. TYPE OF REPORT Scientific No. 23 | 13b. TIME COVERED FROM _____ TO _____ | 14. DATE OF REPORT (Yr., Mo., Day) 1987 March 23 | 15. PAGE COUNT 42 |
| 16. SUPPLEMENTARY NOTATION The work reported herein was performed by The Grumman Corporation under subcontract 86-513 to Center for Space Engineering, Utah State University, Logan, UT 84322-4140. | | | |
| 17. COSATI CODES | | 18. SUBJECT TERMS (Continue on reverse if necessary and identify by block number) | |
| FIELD | GROUP | SUB. GR. | |
| | | Maximum Entropy Method, MEM, Burg, Yule-Walker, FFT, algorithm, signal-to-noise ratio, Lorentzian, data analysis | |
| 19. ABSTRACT (Continue on reverse if necessary and identify by block number) | | | |
| <p>This report summarizes a study of the use of the Maximum Entropy Method (MEM) in processing synthetic and laboratory-obtained interferograms. The capabilities and limitations of the Burg and Y-W MEM algorithms were evaluated and compared to the conventional Fast Fourier Transform (FFT) technique of recovering spectrum from data containing discrete spectral lines.</p> <p>The results showed that the Burg MEM algorithm provided better spectral resolution than the Y-W MEM algorithm. In the absence of unresolved multiple lines, the recovered spectral line width obtained with the Burg MEM was dependent on the line signal-to-noise ratio, the separation of the neighboring lines, and the number of coefficients used. The line shape was consistently a Lorentzian function. The MEM spectral resolution was approximately a factor of two better than the conventional FFT when both correct line strength and line resolution were considered.</p> <p>(cont.)</p> | | | |
| 20. DISTRIBUTION/AVAILABILITY OF ABSTRACT UNCLASSIFIED/UNLIMITED <input checked="" type="checkbox"/> SAME AS RPT. <input type="checkbox"/> DTIC USERS <input type="checkbox"/> | | 21. ABSTRACT SECURITY CLASSIFICATION Unclassified | |
| 22a. NAME OF RESPONSIBLE INDIVIDUAL Francis X. Robert/Contract Monitor | | 22b. TELEPHONE NUMBER (Include Area Code) 617 377-3630 | 22c. OFFICE SYMBOL LSP |

Continued from Block 19:

The time required to compute the coefficient for the MEM algorithm may be prohibitive where near real time recovery of the spectrum is required. The importance of data measurement time versus spectral recovery computational time must be considered for each application of the MEM technique in spectral recovery.

| | |
|--------------------|----------------------|
| For | |
| X | |
| tion | |
| Availability Codes | |
| Dist | Avail and/or Special |
| A-1 | |



FOREWORD

The Air Force Geophysics Laboratory awarded contract number F19628-83-C-0056 to the Center for Space Engineering at Utah State University to assist in their infrared measurement program. Experiments supporting this program measure and characterize infrared emissions from earth, earth limb, upper atmosphere, and deep-space sources. The knowledge gained from these studies increases the understanding of upper atmosphere radiative chemistry and physics and helps to improve surveillance techniques and predictive modeling capabilities.

One program in this contract, the Laboratory Simulation Program, produces a controlled environment data base of molecular interaction infrared emissions from which engineers and planners can refine and improve nuclear and atmospheric predictive codes. An infrared survey experiment conducted under this program involves adapting or fabricating cryogenic infrared sensors to interface with AFGL's LABCEDE facility in support of the overall laboratory simulation program goals.

Yap Analytics, Inc., was awarded Subcontract SC-86-513 obligating them to provide technical support for the LABCEDE program. This support includes investigating the capabilities and limitations of the Maximum Entropy Method (MEM) on interferometric data and using sample laboratory interferometric data to substantiate the results of the investigation.

This document is the final report of their efforts. It summarizes the findings of an investigation into the capabilities and limitations of using the Maximum Entropy Method to process synthetic and laboratory obtained interferograms. Unless otherwise specified, Yap Analytics, Inc., performed the work described in this report.

This page intentionally left blank.

SUMMARY

Yap Analytics, Inc., investigated the use of the Maximum Entropy Method (MEM) in processing synthetic and laboratory-obtained interferograms. The Burg and Y-W MEM algorithms were used in the investigation. The capabilities and limitations of the MEM technique were evaluated and compared to the conventional Fast Fourier Transform (FFT) technique of recovering spectrum from data containing discrete spectral lines.

In this study, the Burg MEM algorithm required a longer computation time than the Y-W MEM algorithm, but provided better spectral resolution and was therefore emphasized in the investigations. The recovered spectral line width obtained with the Burg MEM algorithm was dependent on the line signal-to-noise ratio, the separation of the neighboring lines, and the number of coefficients used. The line width was not a constant function of these parameters when multiple lines, unresolved in the spectral inversion, were present. The line shape, however, was consistently a Lorentzian function.

The MEM spectral resolution was approximately a factor of two better than the conventional FFT when both correct line strength and line resolution were considered. A higher factor of improvement may be realized if only line resolution is desired. However, data interpretation in such an instance may be subject to errors if extreme care is not exercised.

The use of the MEM algorithm necessitates the computation of coefficients in addition to a final FFT inversion. Improper choice of these coefficients can lead to poor resolution, inaccuracies in estimating line strengths, and apparent line splitting as well as additional false lines. The time required to compute the coefficients may be prohibitive for some applications where near real time recovery of the spectrum is required. A search technique may also be required to locate the spectral line peaks after which an integration of the area under the spectral line profiles is necessary to obtain the line strengths. Therefore, the importance of data measurement time versus spectral recovery computational time must be considered for each application of the MEM technique in spectral recovery.

This page intentionally left blank.

TABLE OF CONTENTS

| | <u>Page</u> |
|--|-------------|
| FOREWORD | .iii |
| SUMMARY | v |
| TABLE OF CONTENTS | .vii |
| LIST OF FIGURES | ix |
| LIST OF TABLES | xi |
| 1.0 INTRODUCTION | 1 |
| 2.0 SYNTHETIC DATA STUDIES | 3 |
| 2.1 Synthetic Data and Noise | 3 |
| 2.2 FFT Spectral Recovery | 4 |
| 2.3 Burg vs Y-W | 4 |
| 2.4 Line Profile | 4 |
| 2.5 Line Width | 8 |
| 2.6 Line Peak Shift | 8 |
| 2.7 Two Line Resolution | 12 |
| 2.8 Multiple Line Resolution | 13 |
| 2.9 Rectangular and Triangular Spectra | 13 |
| 3.0 LABORATORY DATA | 17 |
| 3.1 FFT Results | 17 |
| 3.2 Burg MEM Results | 21 |
| 3.3 Y-W MEM Results | 24 |
| 4.0 SUMMARY AND CONCLUSIONS | 27 |
| REFERENCES | 29 |

This page intentionally left blank.

LIST OF FIGURES

| <u>Figure</u> | | <u>Page</u> |
|---------------|---|-------------|
| 1 | Synthetic Interferogram and Noise | 5 |
| 2 | FFT Recovered PSD of Synthetic Interferogram | 5 |
| 3 | Recovered PSD of Synthetic Interferogram with Burg MEM | 6 |
| 4 | Recovered PSD of Synthetic Interferogram with Y-W MEM | 6 |
| 5 | MEM Recovered PSD Area | 7 |
| 6 | MEM Recovered PSD Line Width | 9 |
| 7 | MEM Recovered PSD Line Width | 10 |
| 8 | MEM Recovered PSD Line Width | 11 |
| 9 | PSD Line Peak Shift Recovered with MEM | 12 |
| 10 | Five Equal Strength Lines Recovered with FFT | 14 |
| 11 | Five Equal Strength Lines Recovered with MEM and Integrated . . . | 14 |
| 12 | Two Unequal Rectangles Recovered with FFT | 15 |
| 13 | Two Unequal Rectangles Recovered with MEM | 15 |
| 14 | Two Unequal Triangles Recovered with FFT | 16 |
| 15 | Two Unequal Triangles Recovered with MEM | 16 |
| 16 | LABCEDE Interferogram '4d19d' | 18 |
| 17 | LABCEDE Interferogram Recovered with FFT | 18 |
| 18 | LABCEDE Interferogram Recovered with FFT - Band 1 | 19 |
| 19 | LABCEDE Interferogram Recovered with FFT - Band 2 | 19 |
| 20 | 800 Points of LABCEDE Interferogram Recovered with FFT | 20 |
| 21 | 600 Points of LABCEDE Interferogram Recovered with MEM | 22 |
| 22 | 600 Points of LABCEDE Interferogram Recovered with MEM and Integrated - Band 1 | 23 |
| 23 | 600 Points of LABCEDE Interferogram Recovered with MEM and Integrated - Band 2 | 23 |
| 24 | 1000 Points of LABCEDE Interferogram Recovered with MEM | 25 |
| 25 | 600 Points of LABCEDE Interferogram Recovered with Y-W MEM . . . | 25 |

This page intentionally left blank.

LIST OF TABLES

| <u>Table</u> | | <u>Page</u> |
|--------------|-------------------------|-------------|
| 1 | Summary of FFT Results | 20 |
| 2 | Summary of Burg Results | 22 |
| 3 | Summary of Y-W Results | 24 |

This page intentionally left blank.

1.0 INTRODUCTION

The Maximum Entropy Method (MEM) has been widely applied in areas where super-resolution of measured data spectrum is required. Super-resolution refers to obtaining a much higher resolution of the data than permitted by the conventional Fast Fourier Transform (FFT) technique because of the limited measured data length. Numerous articles¹⁻⁴ on the topic, including comparisons of various MEM algorithms, may be found in the open literature. However, the theoretical capabilities and limits of the MEM technique in processing data known to contain closely spaced spectral lines of variable line spacings have not been reported. Such results are important to spectroscopic data processing. This investigation was therefore directed to the behavior of the MEM algorithm, its capabilities and improvements over the conventional FFT method, and its limitations in processing this special class of data.

One prime advantage of the MEM technique over the conventional FFT method in recovering the spectrum is the absence of lobes in the wings of the recovered spectrum that often accompany FFT processing due to the mathematical artifact of data 'windowing'. This reduces the chances of error in data spectral analysis and misinterpretation of false lines, as well as the chances of losing lines due to the camouflage by the wings of neighboring lines of much higher intensity. However, this advantage holds only if the proper number of MEM coefficients, consistent with the data resolution, are used in the processing. Improper choice of the MEM coefficients often leads to poor resolution, inaccuracies in estimating line strengths, and the apparent line splitting as well as additional false lines.

The interferogram is the autocorrelation of the input source radiation because of the square law behavior of the detector. As such, the Yule-Walker (Y-W) MEM algorithm would be particularly suited to its application. The Y-W in general requires less computation time. However, the Burg algorithm generally provides better spectral resolution. With the Burg algorithm, the interferogram is treated as the time series rather than an autocorrelation. A longer computation time is required with the Burg than with the Y-W.

In this study, the MEM technique was used to process synthetic and laboratory-obtained data. Both sources of data contained spectral lines of varying signal-to-noise ratios (SNR) and varying line spectral separations. The results of the MEM technique were compared to results obtained with the FFT technique, and the capabilities and limitations of the MEM technique were evaluated. Both the Burg and the Y-W MEM algorithms were used in the investigations.

2.0 SYNTHETIC DATA STUDIES

The MEM algorithm was first applied to synthetic line data to investigate its capabilities and limitations. The generation of the synthetic data and the results of the investigation are described in the following sections.

2.1 SYNTHETIC DATA AND NOISE

A pseudo-random white Gaussian noise was produced from an algorithm. The following algorithm generates a set of uniformly distributed white spectral random numbers from a recursive equation:

$$X_{n+1} = (aX_n + c) \text{ mod } m \quad (1)$$

where,

$$X_0 = \text{seed}$$

$$a = 24298$$

$$c = 99991$$

$$m = 199017$$

The generated numbers, X_n , range from 0 to 1 and if pairs of these numbers are used in the following equation,

$$X = \text{Sqrt}(-2 \ln U_1) \cos (2\pi U_2) \quad (2)$$

where U_1 and U_2 are pairs of random numbers generated from Equation (1), a Gaussian distributed white noise of unit standard deviation and zero mean results. An array of 512 points of noise was created by this algorithm.

A 512 point interferogram of artificial data lines was then theoretically created. Each line was represented by a cosine waveform to simulate the output of an interferometer. Each line may be scaled individually for signal strength, and lines at various spectral frequencies and line spacings may be generated. The unit standard deviation Gaussian white noise was then added to the interferogram. A sample of the synthetic line data with noise is illustrated in Figure 1. The sample spacing was arbitrarily chosen to be 0.0001953 second. The interferogram contained two lines of frequencies 1260.00 and 1280.00 and SNRs of 6 and 12, respectively.

2.2 FFT SPECTRAL RECOVERY

The interferogram of Figure 1 has a 'window' width of 0.1 second. The spectral resolution afforded by the conventional FFT method of recovery is 20.0 Hz, i.e., the first zero crossing of the spectral line profile is 10.0 Hz and two lines must be separated by 20.0 Hz to be unambiguously resolved. To demonstrate the integrity of the FFT technique of recovering the line strengths, a 1024 point interferogram was used for the inversion (corresponding to spectral resolution of 10.0 Hz). The interferogram was further 'zero padded' for finer spectral computational resolution. The recovered power spectrum, shown in Figure 2, preserved the proper line strength ratios of 0.25:1 in power (0.5:1 in input radiance). Had the original 512 point interferogram been used instead, there would have been a small amount of spectral cross-talk affecting both the locations as well as the peaks of both lines, more strongly for the lower amplitude line.

2.3 BURG VS Y-W

This quick comparison was exercised to justify the use of the Burg instead of the Y-W algorithm. Two equal intensity lines with a spacing of 20.0 Hz were recovered using the Burg and the Y-W algorithms and the results are shown in Figures 3 and 4. In each case, 64 coefficients were computed and used in the spectral inversion. In the Power Spectral Density (PSD) plot of Figure 3, recovered with the Burg algorithm, the two lines were distinctly resolved but in the PSD plot of Figure 4, recovered with the Y-W algorithm, the two lines were not distinctly separated. The area under each line in the PSD curve was found to be consistently equal to the corresponding input line power for both algorithms as long as the lines were distinctly separate. The Burg algorithm was thus selected for the major portion of the investigation.

2.4 LINE PROFILE

The interferogram of a single line was used to quantitatively evaluate the line profile obtained with the Burg algorithm. The line frequency was chosen to be approximately in the mid range of the computed spectral display. For the 512 point interferogram, the normalized output Nyquist frequency was 256. The line frequency was set at 126.

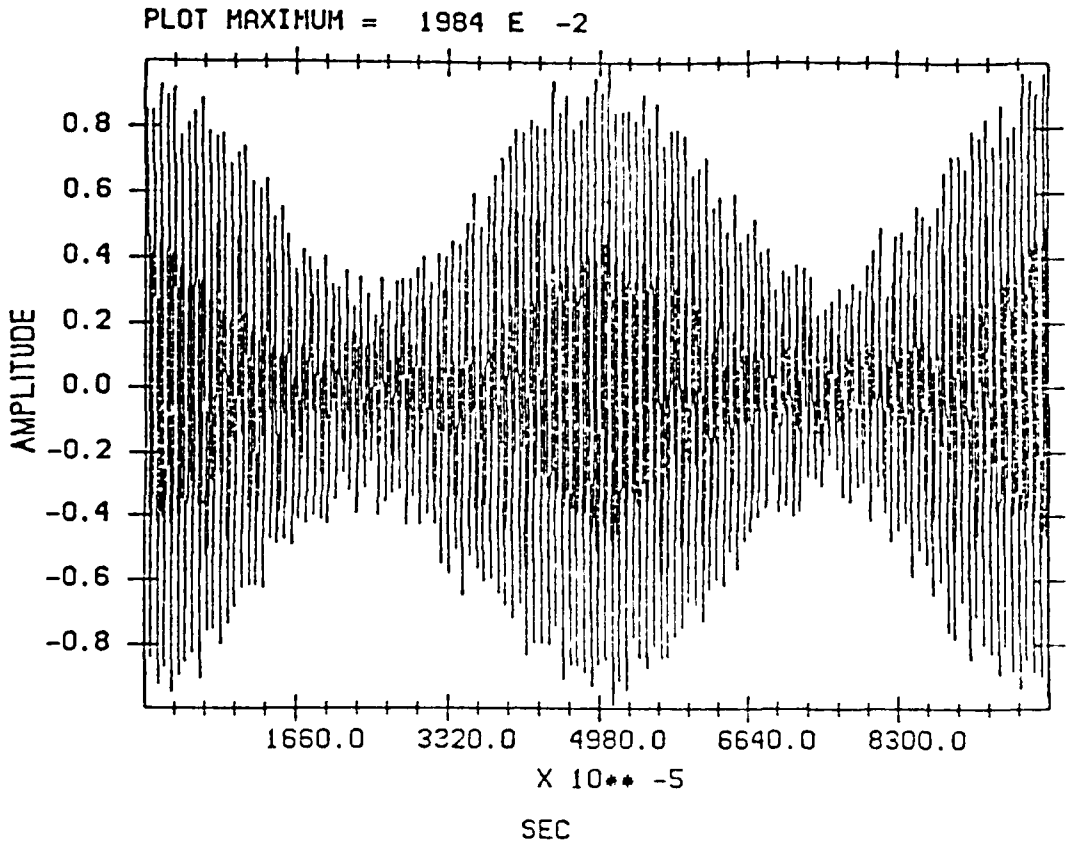


Figure 1. Synthetic Interferogram and Noise.

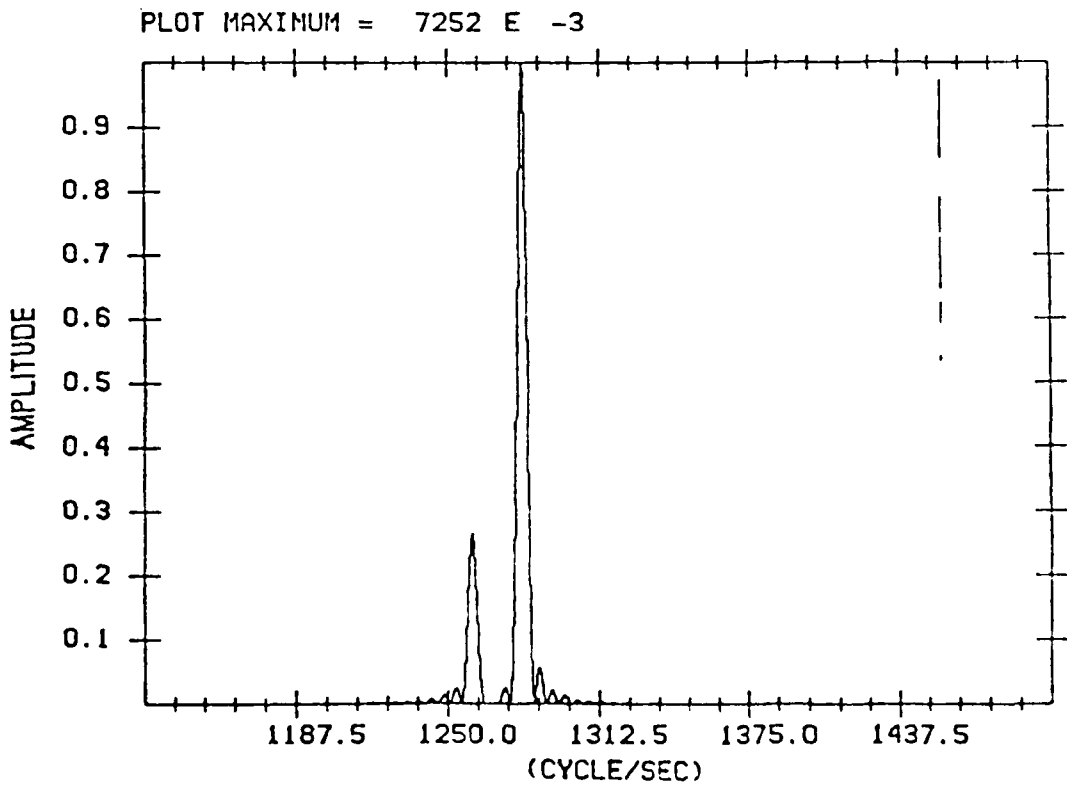


Figure 2. FFT Recovered PSD of Synthetic Interferogram.

PSD - BURG MEM - 64

PLOT MAXIMUM = 3638 E -3

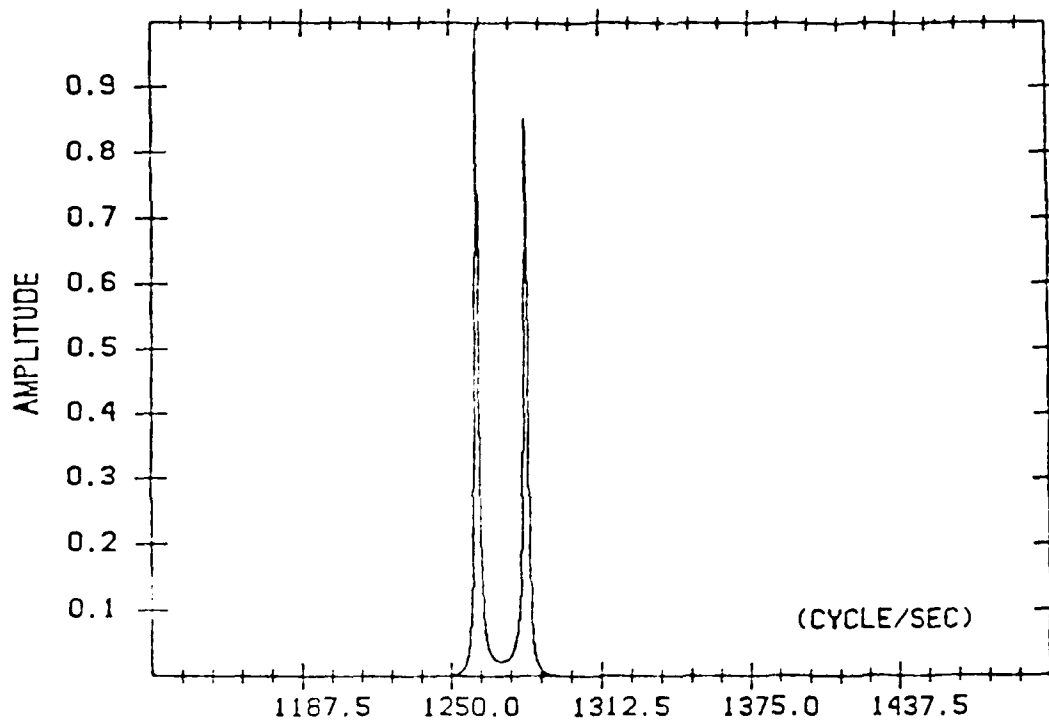


Figure 3. Recovered PSD of Synthetic Interferogram with Burg MEM.

PSD - YW MEM - 64

PLOT MAXIMUM = 488 E -3

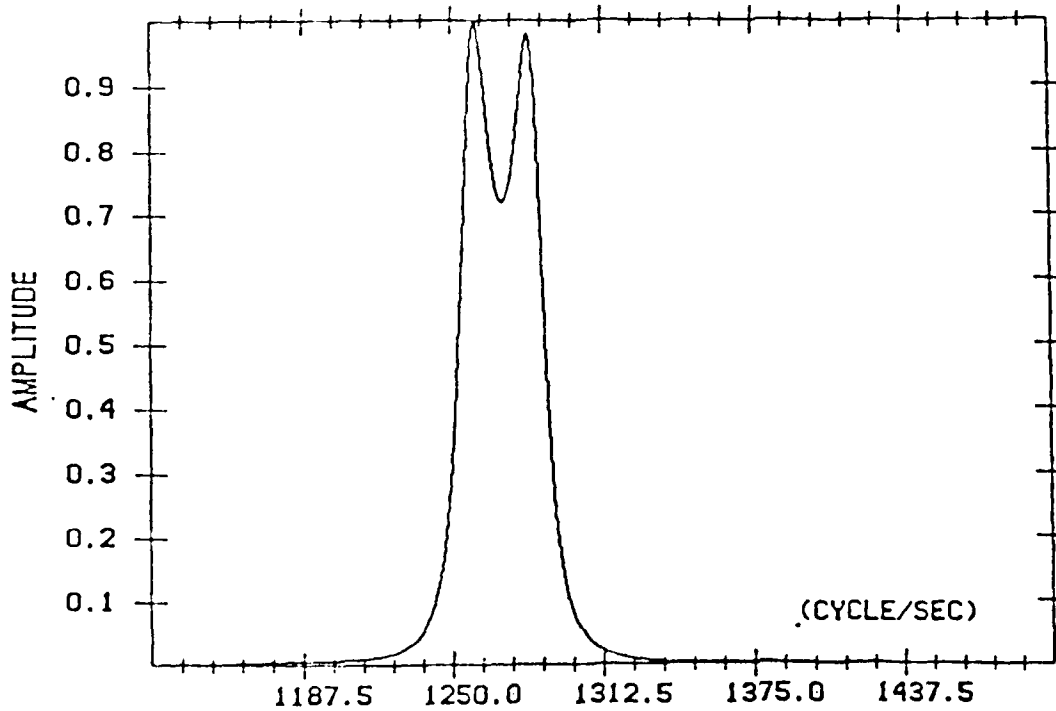


Figure 4. Recovered PSD of Synthetic Interferogram with Y-W MEM.

Using 64 coefficients for the inversion, the area under the PSD curve was integrated between symmetric points of the line peak. Figure 5 shows plots of the integrated PSD area versus the limits of integration as a fraction of the PSD peak value. The integrated areas were normalized by 100 and only the positive frequency line was used. Three SNRs (18, 12, and 6) were used. The top curve shows the integrated area for a theoretical Lorentzian function for comparison. It appeared that the MEM line profile was approximately a Lorentzian independent of SNR.

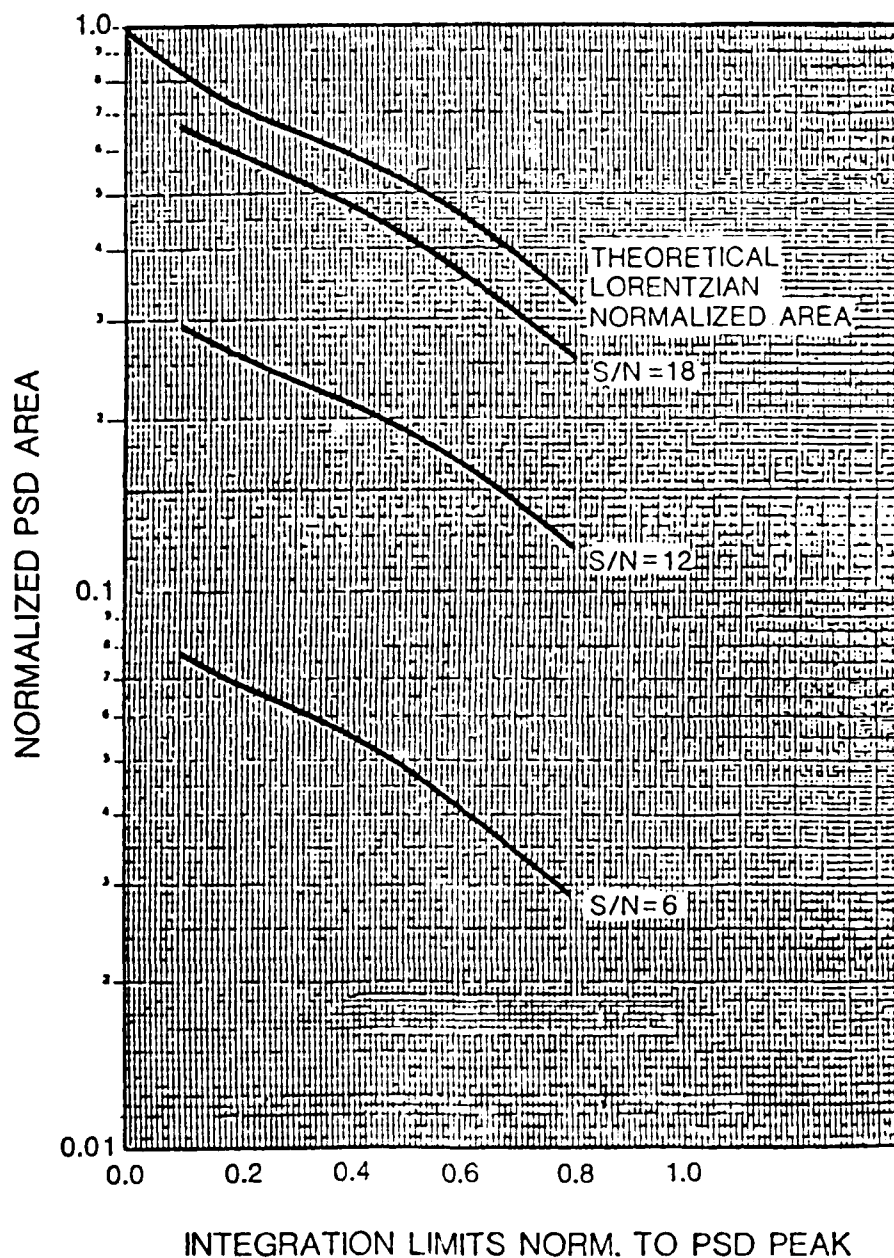


Figure 5. MEM Recovered PSD Area.

2.5 LINE WIDTH

The line width for a single line obtained with the Burg algorithm was next investigated. The line width was arbitrarily determined by locating the 10% points of the PSD line peak. Figures 6 through 8 illustrate the behavior of the line width as the number of coefficients as well as the SNR were varied. Three normalized frequencies at 240, 128, and 32 are shown in the respective figures. The plotted line widths were normalized to the conventional FFT line width consistent with the interferogram length. For small numbers of coefficients, the line width was inversely proportional to the square of the SNR and rather independent of line frequency. The line width appeared to be linearly proportional to the inverse of the number of coefficients for small number of coefficients and low SNRs.

The above observations were qualitatively found to be true for multiple lines as long as the lines were sufficiently separated to be distinctly resolved. However, the linearity fell apart when two or more lines were not distinctly resolved.

2.6 LINE PEAK SHIFT

The effect of line peak shifting, reported by Chen et al⁵, was investigated. The line frequency was decreased and the PSD line peak was found using a search routine. For this investigation, 64 coefficients were used in the inversion. The results of Chen were duplicated (Figure 9) except for the phase reversal (probably due to the difference in shift definition). When the interferogram contained an integer number of quarter cycles of the waveform, the normalized line shift was zero. The sinusoidal interferogram must also begin either at the peak or zero, as Chen observed, for the above to be true. The normalized line shift increased as the frequency decreased becoming very severe when the interferogram contained less than one cycle of the waveform. The area under the PSD curve varied with the frequency corresponding to the input line power (i.e., power was preserved).

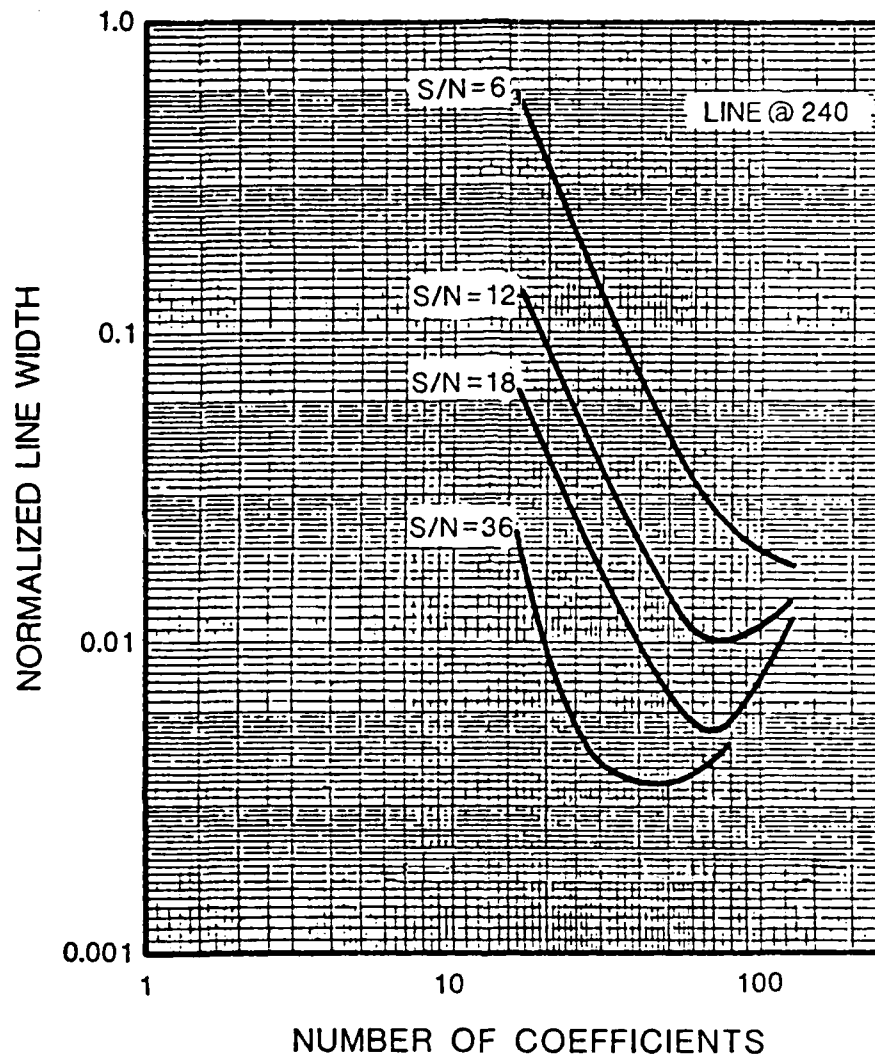


Figure 6. MEM Recovered PSD Line Width.

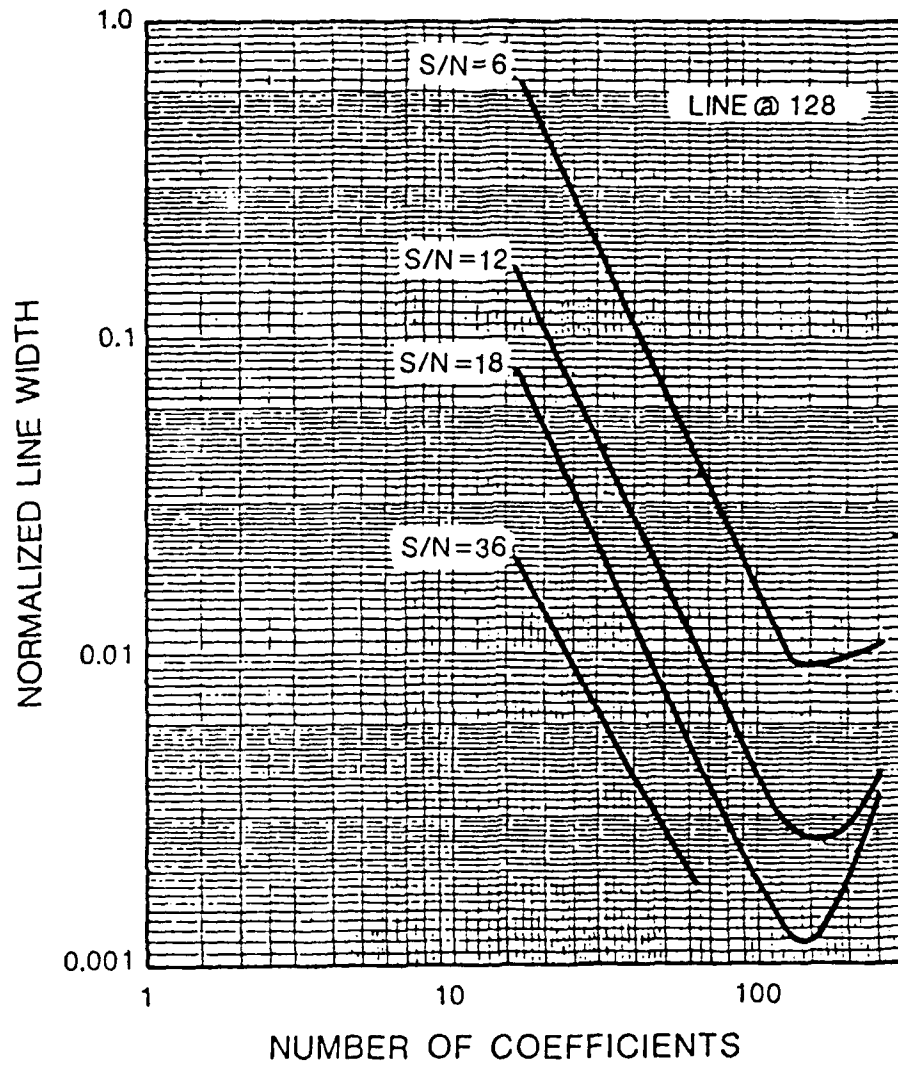


Figure 7. MEM Recovered PSD Line Width.

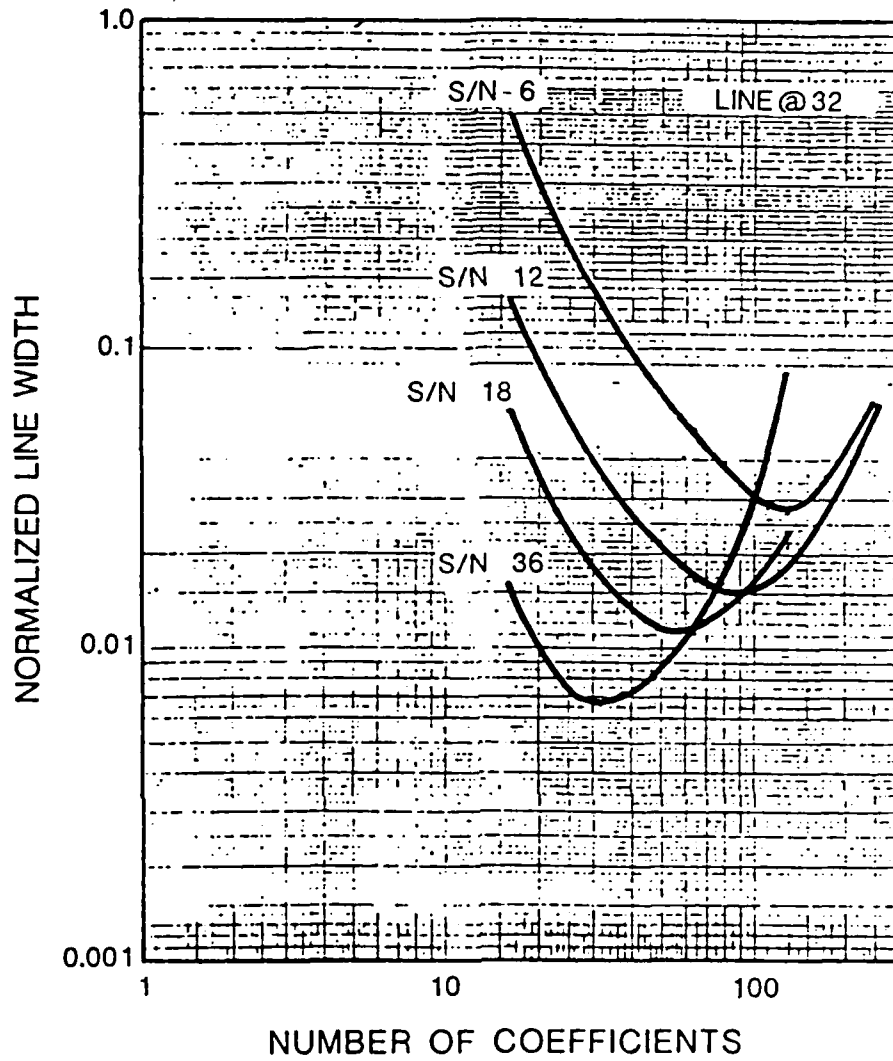


Figure 8. MEM Recovered PSD Line Width.

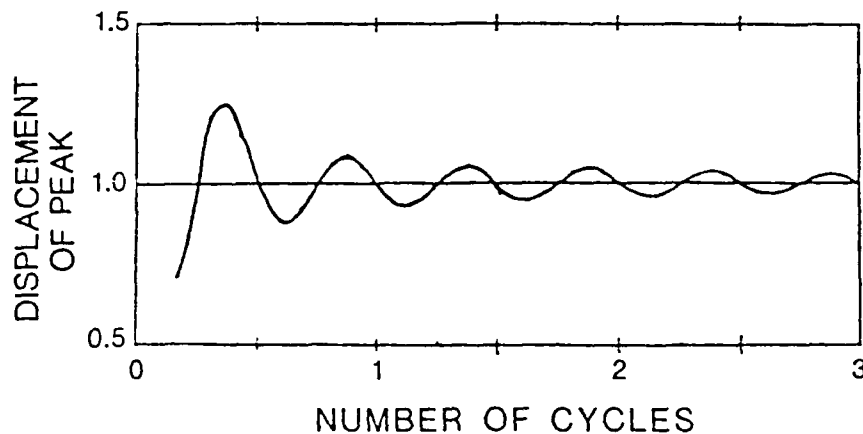


Figure 9. PSD Line Peak Shift Recovered with MEM.

The effect also manifested itself for interferograms with two spectral lines. Whenever the 'beat' frequency of the two lines were not equal to an integer number of quarter cycles in the interferogram, an error in line locations resulted. The effect became less severe (i.e., the fractional shift decreased) as the line frequencies increased far beyond the 'beat' frequency. Correlating with the line shifts were errors in estimating line strength ratios, although the sum of the output power of the lines was always equal to the input power of the lines.

2.7 TWO-LINE RESOLUTION

The all-important question of the ultimate resolution of the MEM for two spectral lines was investigated next. The rules were that the two-output line strength ratio should be recovered to within 90% of the input line ratio without spurious lines being created. A SNR of 6 for each line was used in this study. The two-line 'beat' frequency was held constant as the number of MEM coefficients was varied to find the optimum. The 'beat' frequency was then decreased and the optimum number of coefficients again located. It was found that the ultimate resolution of the Burg MEM was a factor of two better than the conventional FFT. In order to resolve two lines separated by one wave-number and preserve the line strength ratios, an interferogram of one centimeter retardation was necessary.

2.8 MULTIPLE LINE RESOLUTION

An interferogram of five lines with equal SNR of 12 was synthesized as described previously. A spectrum recovered with the conventional FFT algorithm on a 1024 point interferogram (corresponding to a normalized resolution of 1 point in the spectrum) is shown in Figure 10. The spectrum recovered with the Burg algorithm on a 512 point interferogram is shown in Figure 11. Here the area under each PSD spectral line curve was searched and integrated. The PSD was then replaced by the integrated areas at the frequencies where the peaks were found. The recovered spectra of Figures 10 and 11 were comparable in line ratio variation, showing again that the Burg algorithm was a factor of two better than the FFT algorithm even for multiple line spectra.

2.9 RECTANGULAR AND TRIANGULAR SPECTRA

An interferogram of two rectangular spectra of unequal SNR was synthesized. The FFT and the Burg algorithms were used to recover the spectra. Figures 12 and 13 show the spectra recovered. Figures 14 and 15 show the recovered spectra of two unequal SNR triangular input spectra recovered with the FFT and Burg algorithm. Figures 13 and 15 appear to indicate that the MEM algorithm may not be suitable for these types of spectra.

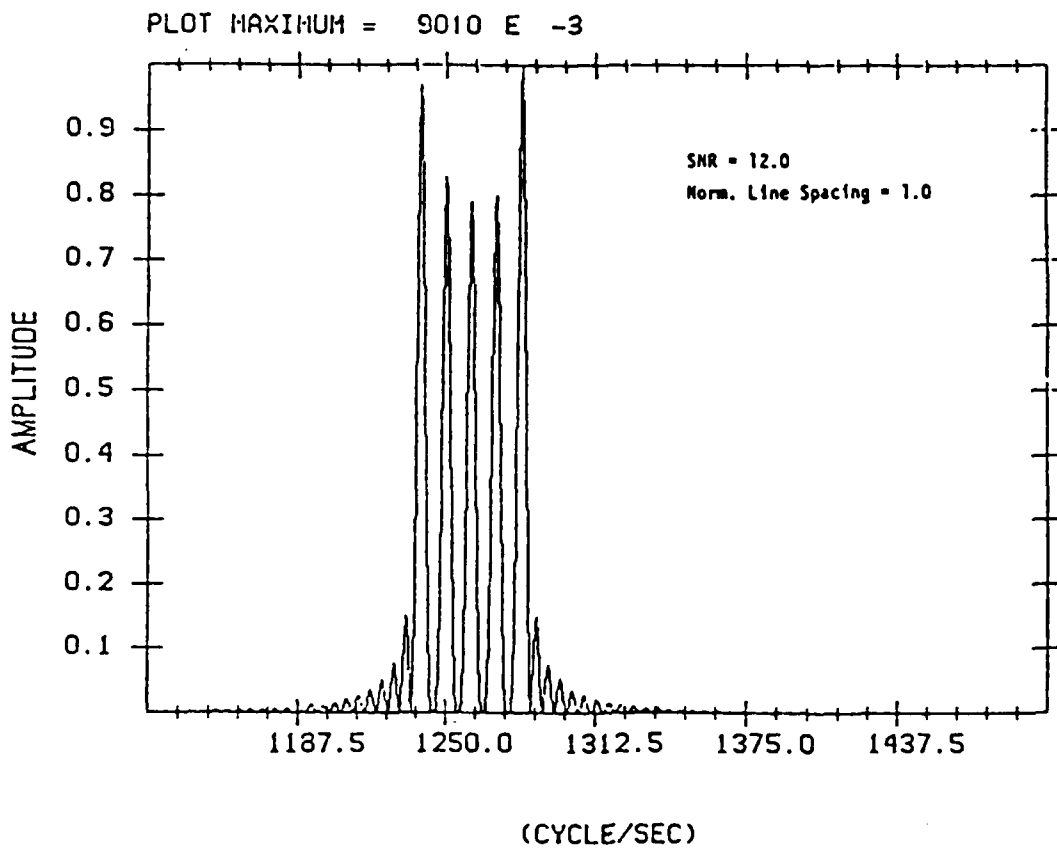


Figure 10. Five Equal Strength Lines Recovered with FFT

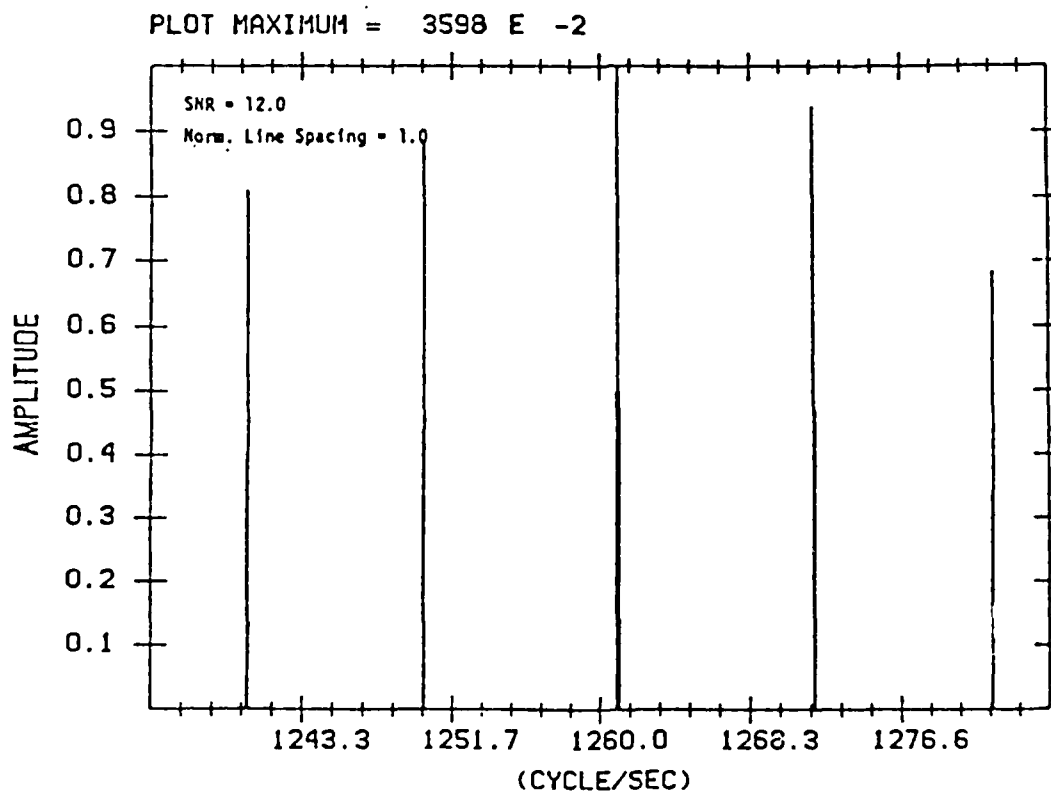


Figure 11. Five Equal Strength Lines Recovered with MEM and Integrated.

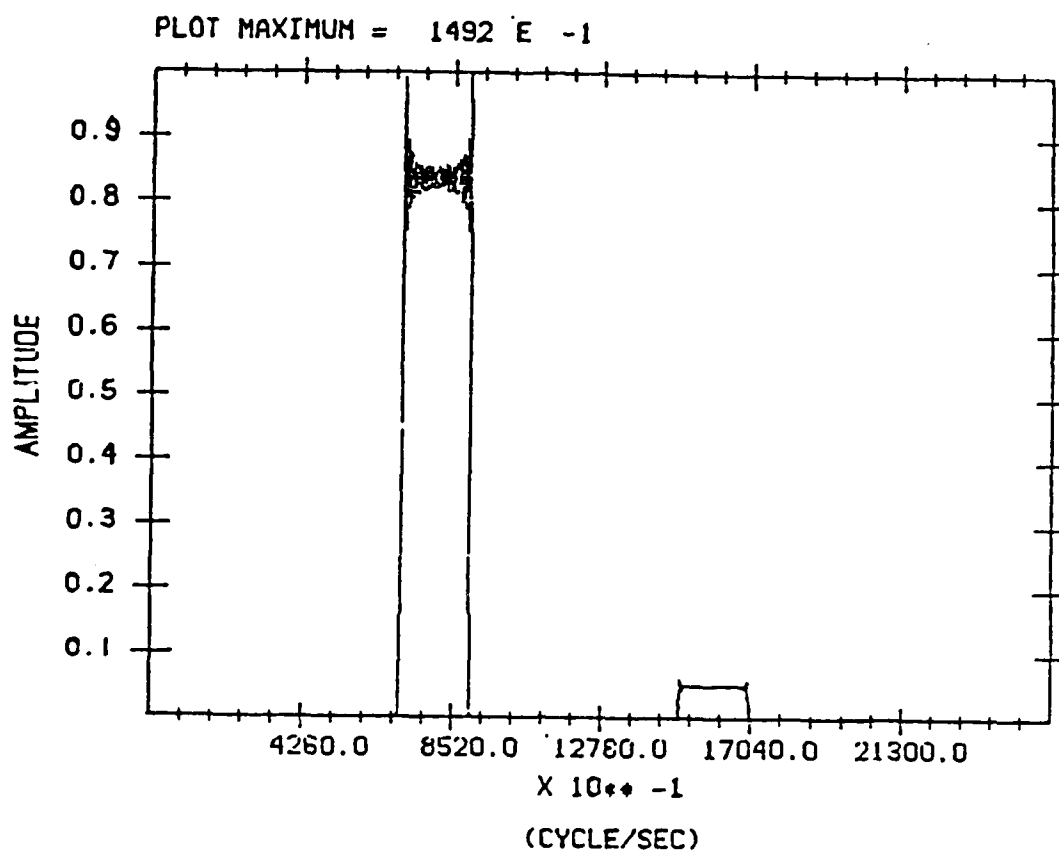


Figure 12. Two unequal Rectangles Recovered with FFT.

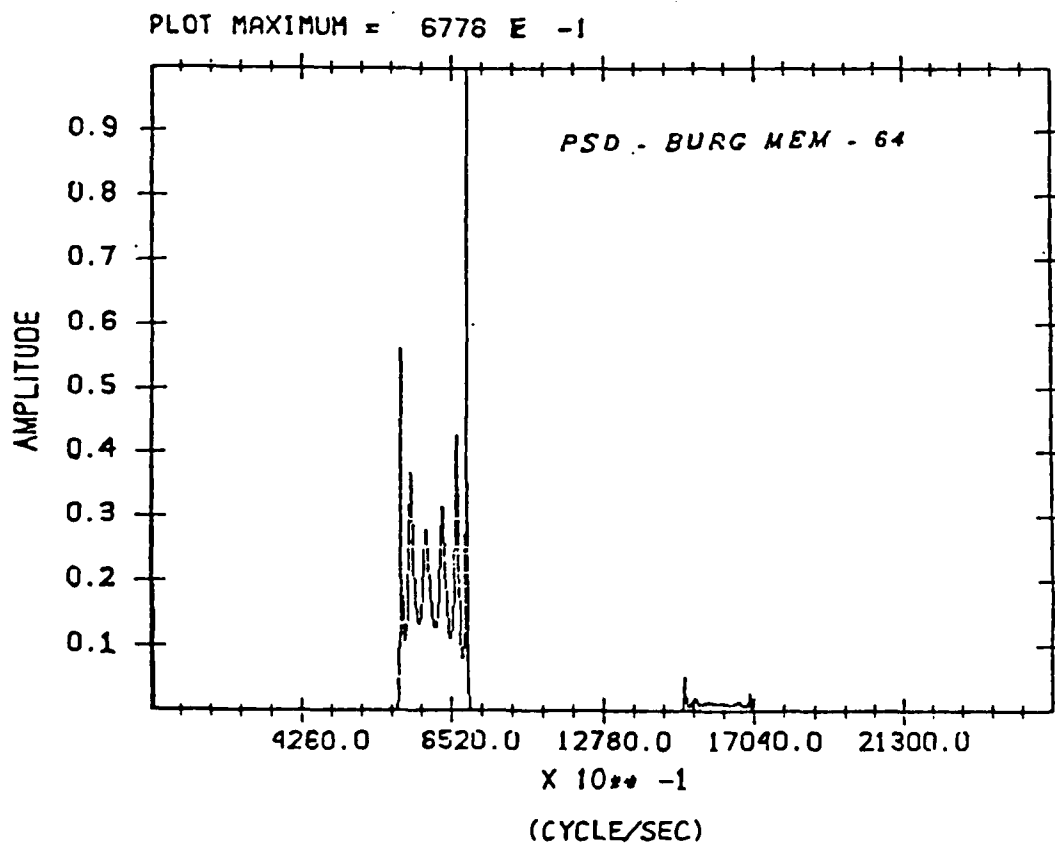


Figure 13. Two Unequal Rectangles Recovered with MEM.

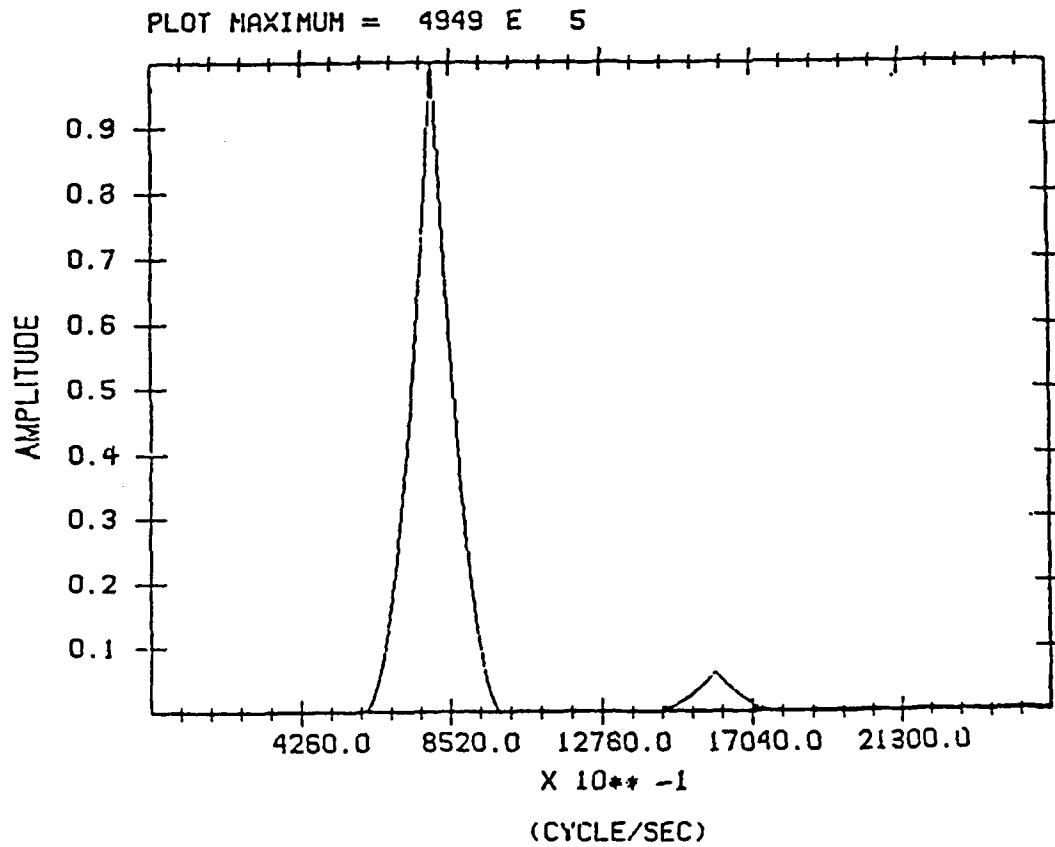


Figure 14. Two Unequal Triangles Recovered with FFT.

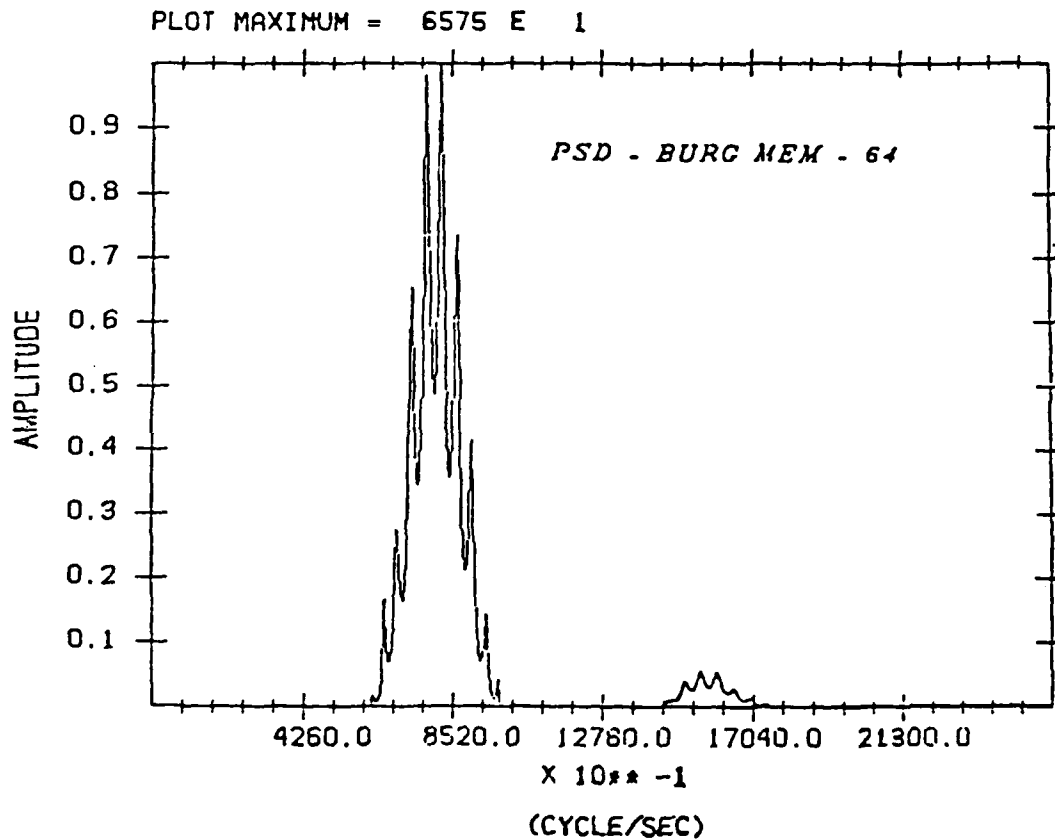


Figure 15. Two Unequal Triangles Recovered with MEM.

3.0 LABORATORY DATA

The investigation was then extended to the LABCEDE measured laboratory data. The 32nd scan of the interferogram labelled '4d19d' (Figure 16) was used for the study. The interferogram contained 2350 points of data sampled at 0.6328 micrometers. If the full interferogram was used in the conventional FFT technique, the first zero crossing of the line profile would be 6.7 wavenumbers. The instrument's conventional resolution is therefore 13.5 wavenumbers. A spectrum, recovered with a 'zero padded' 8K FFT on the 2350 point interferogram, is shown in Figure 17 containing multiple lines. Two spectral regions were selected for further investigation: 1800 to 2000 wavenumbers and 2700 to 2800 wavenumbers, shown expanded in Figures 18 and 19, respectively. The first spectral band contained four strong lines at approximately 1727, 1809, 1890 and 1955 wavenumbers. The other band contained two strong lines at approximately 2738 and 2778 wavenumbers. The closest line spacing in each band was approximately 31 wavenumbers.

3.1 FFT RESULTS

The interferogram length was truncated symmetrically around its peak and its spectrum magnitude was obtained using the conventional FFT technique. No apodization on the interferogram was used. Table 1 shows the six line peaks obtained as the interferogram length was shortened. The second column indicates the theoretical first zero crossing of the FFT algorithm. The third column shows the peak value of the line at 1809 wavenumbers. The next three columns are the line peaks of the first band normalized to the line peak at 1809 wavenumbers. The line peak at 2778 wavenumbers is shown in the next column. The last column shows the 2738 wavenumber line peak normalized to the peak at 2778 wavenumbers.

Table 1 shows the basic limitations of the FFT algorithm. The line strengths were preserved until the interferogram length was shortened to the point where the lines were not resolved. Figure 20 illustrates this point - when the interferogram was shortened to 800 points corresponding to 40 wavenumber resolution with the conventional FFT algorithm, errors in the output spectral amplitudes were observed for the two closely spaced lines in both bands.

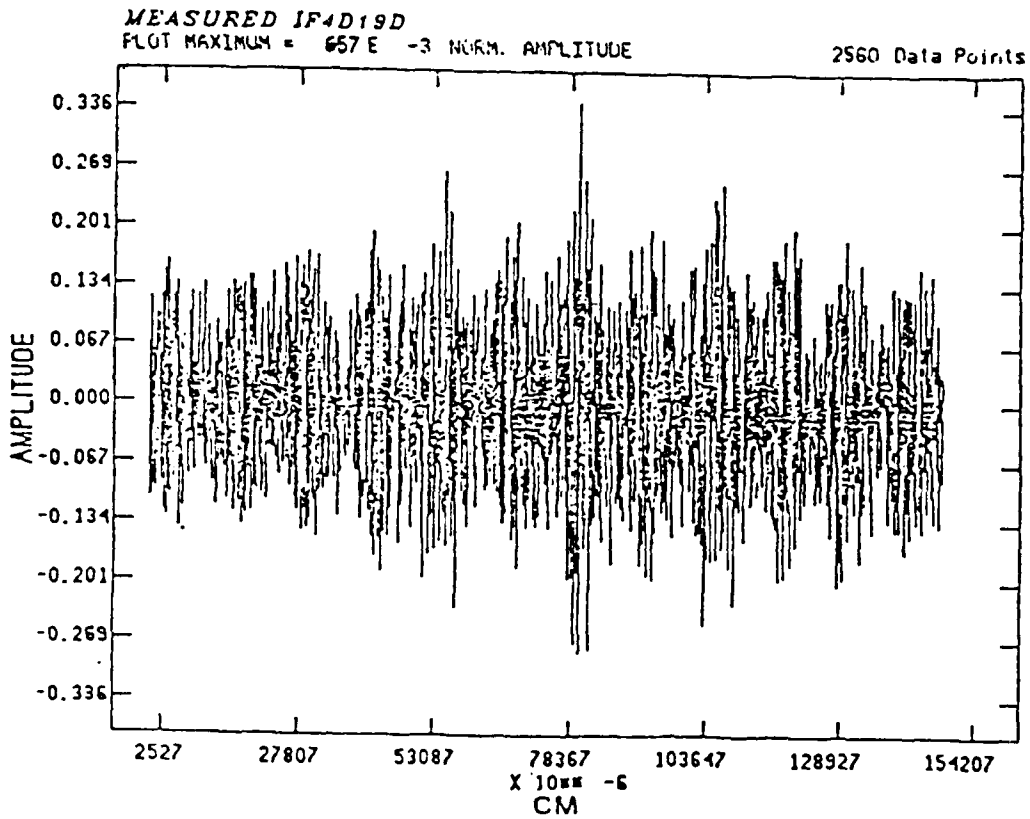


Figure 16. LABCEDE Interferogram '4d19d'

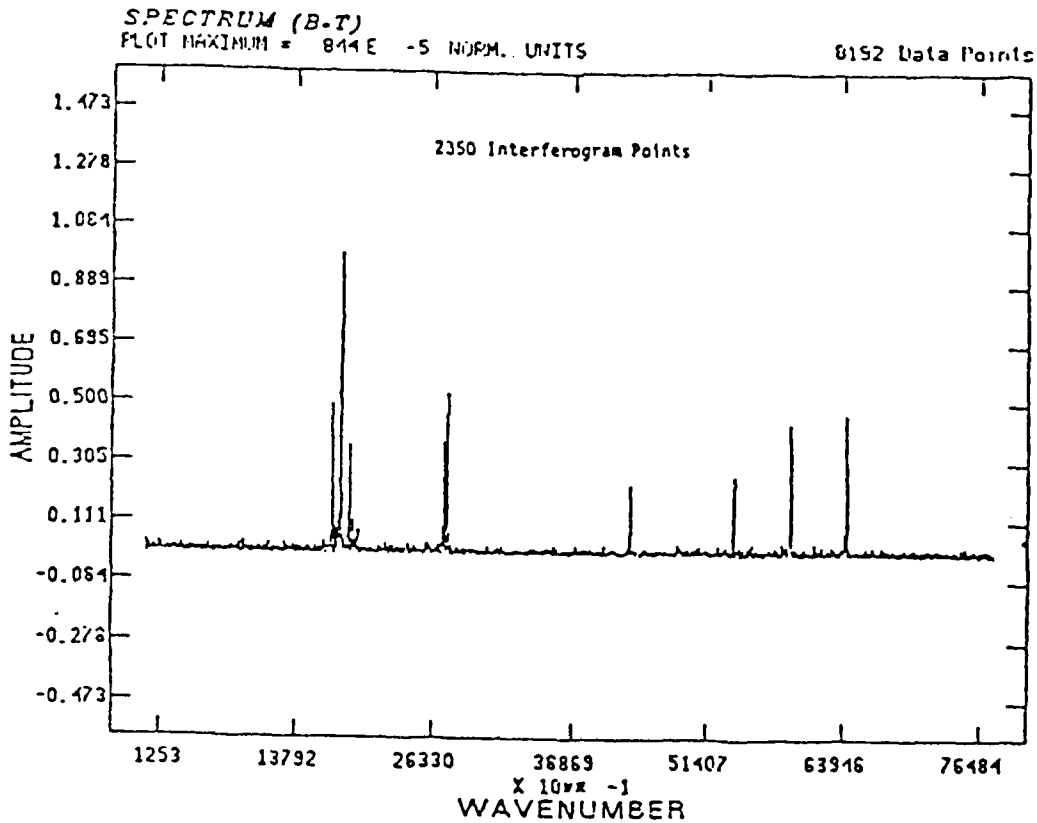


Figure 17. LABCEDE Interferogram Recovered with FFT.

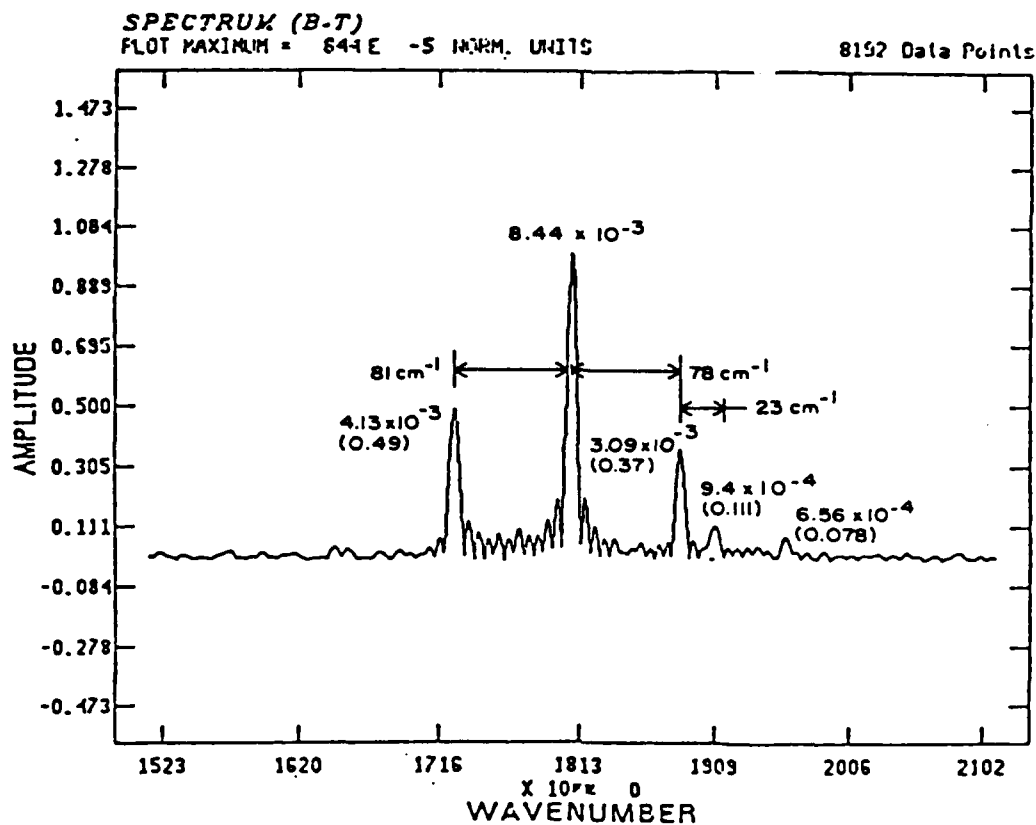


Figure 18. LABCEDE Interferogram Recovered with FFT - Band 1

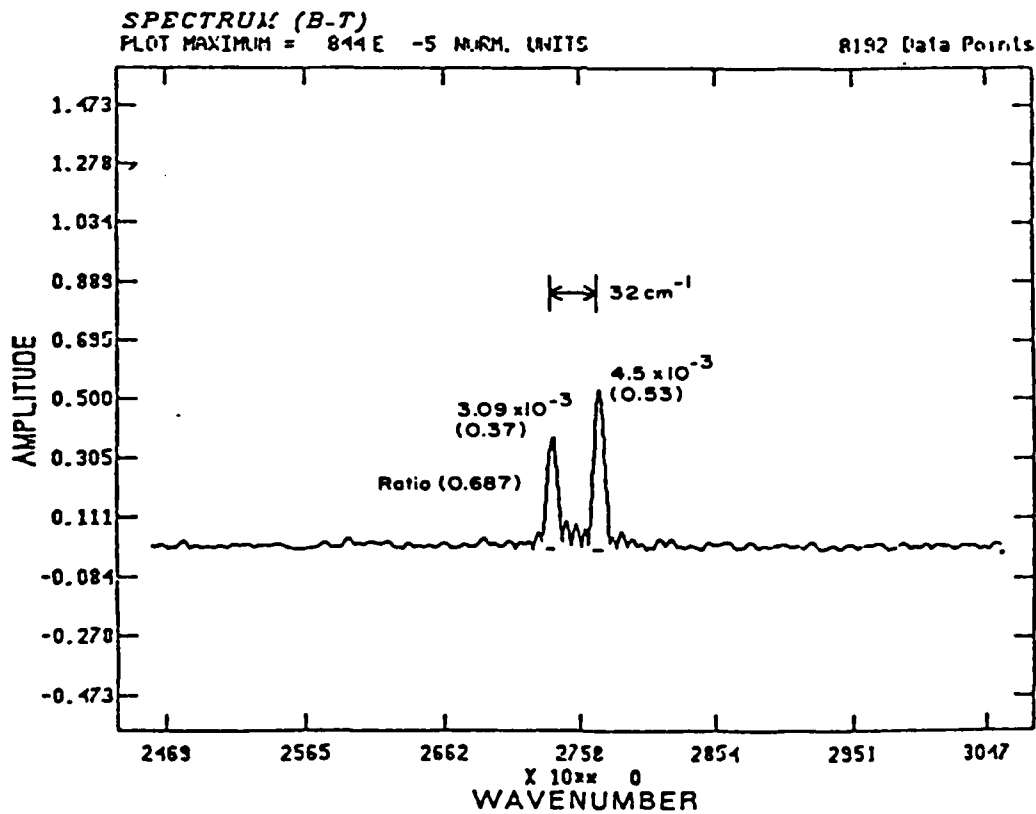


Figure 19. LABCEDE Interferogram Recovered with FFT - Band 2

TABLE 1 Summary of FFT Results
(Squareroot PSD(f))

| # IF Points | 1st Zero Crossing (cm^{-1}) | Line Peak 1809 (cm^{-1}) | Norm. Line Peak | | | Line Peak 2778 | Norm. Line Peak 2738 (cm^{-1}) |
|-------------|--|-------------------------------------|-----------------|------|-------|----------------|---|
| | | | 1727 | 1890 | 1955 | | |
| 2350 | 6.7 | 0.00844 | 0.49 | 0.37 | 0.111 | 0.0045 | 0.687 |
| 1000 | 15.8 | 0.005689 | 0.47 | 0.37 | 0.111 | 0.0037 | 0.668 |
| 800 | 20.0 | 0.005025 | 0.54 | 0.37 | 0.106 | 0.00324 | 0.509 |
| 600 | 26.0 | 0.00436 | 0.52 | 0.39 | 0.08 | 0.00257 | unresolved |
| 400 | 40.0 | 0.00371 | 0.56 | 0.51 | 0.21 | 0.00285 | " |
| 300 | 53.0 | 0.002775 | unresolved | | | 0.002775 | " |

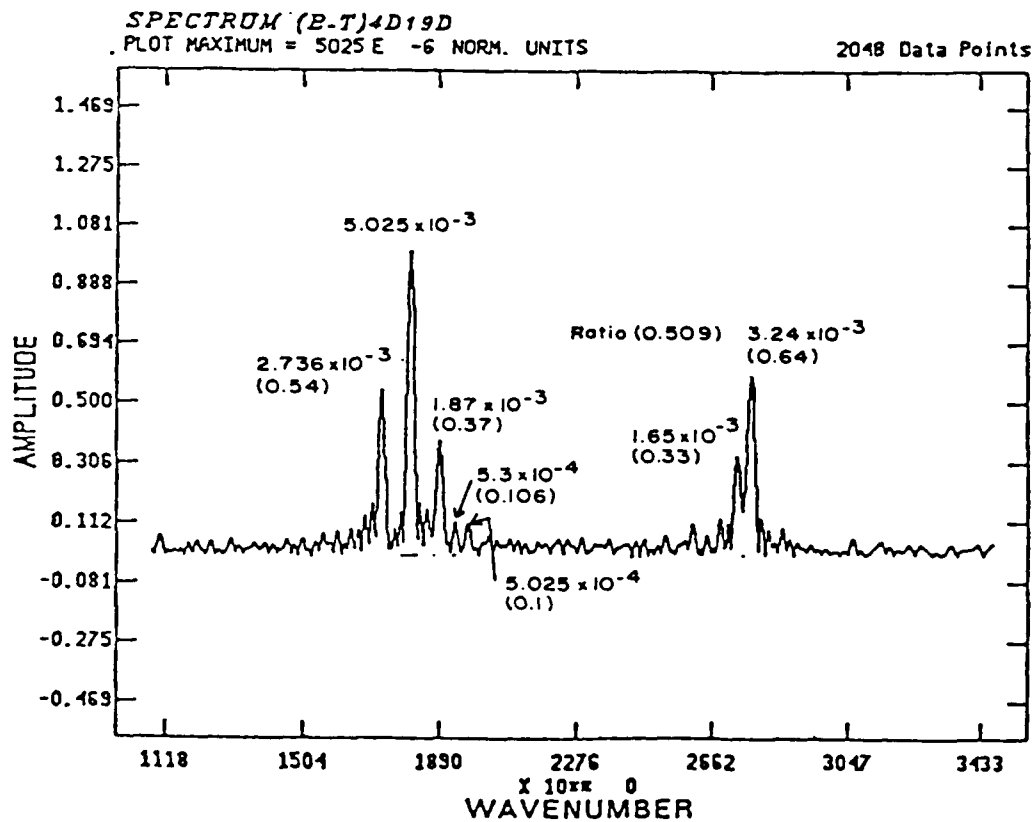


Figure 20. 800 Points of LABCEDE Interferogram Recovered with FFT.

3.2 BURG MEM RESULTS

The procedure of Section 3.1 was then repeated with the Burg algorithm. For each symmetrically truncated interferogram, a set of MEM coefficients were computed. The PSDs were then inverted from the coefficients with a FFT routine. A sample of the recovered spectrum (square root of the PSD) using 240 coefficients on the 600 point symmetric interferogram is shown in Figure 21. Notice the line PSD peak ratios at this stage are generally not equal to the input line ratios. The PSDs were then searched in the two bands to locate spectral peaks. An integration of the line power was then performed after which its square root was obtained. The PSD curve was then replaced by the integrated values at the locations of the peaks. The final spectra of the two bands are shown in Figures 22 and 23. This is a common practice and sometimes presents the wrong impression of the infinite resolution of MEM processing. One must, however, bear in mind that the spectra of Figures 22 and 23 were not the results of merely utilizing the MEM algorithm but that they had been further processed. Table 2 tabulates the results obtained. The format is the same as Table 1 except for the insertion of an extra column indicating the number of coefficients used in the inversion. Notice the PSD line areas in Table 2 are approximately equal to the spectral peaks in Table 1 times the square root of the indicated first zero crossings, as theoretically expected. Comparison of Tables 1 and 2 leads to the conclusion that the Burg MEM required half the interferogram length to achieve the same resolution as the conventional FFT algorithm.

It was found that the optimum number of coefficients was consistently approximately 40-60% of the interferogram length. As the number of coefficients were increased, spurious lines began to appear as shown in Figure 24.

TABLE 2 Summary of Burg Results
(Squareroot / PSD(f_0)df)

| # IF Points | 1st Zero Crossing (cm ⁻¹) | # Coef. | Line Area | | Norm. Line Area | | Area | Norm. Area |
|-------------|---------------------------------------|---------|--------------------------|--------------------------|-----------------|--------------------------|----------------|------------|
| | | | 1809 (cm ⁻¹) | 1727 (cm ⁻¹) | 1890 | 2778 (cm ⁻¹) | 2738 | |
| 1000 | 15.8 | 400 | | | | | 0.0126 | 0.623 |
| | | 600 | | | | | 0.01329 | 0.574 |
| | | 800 | | | | | Line Splitting | |
| 800 | 20.0 | 320 | 0.0205 | 0.507 | 0.36 | | | |
| 600 | 26.0 | 240 | 0.02016 | 0.530 | 0.39 | 0.01225 | 0.585 | |
| | | 360 | | | | 0.01225 | 0.582 | |
| 500 | 31.6 | 250 | 0.0218 | 0.5 | 0.394 | 0.01197 | 0.80 | |
| | | 300 | | | | 0.01195 | 0.0798 | |
| 400 | 40.0 | 160 | 0.02073 | 0.49 | 0.455 | | | |
| | | 240 | 0.02058 | 0.48 | 0.456 | 0.01629 | 0.35 | |
| | | 320 | | | | 0.01652 | 0.345 | |
| 200 | 79.0 | 100 | 0.0189 | 0.735 | 0.467 | | | |
| | | 140 | 0.0206 | 0.74 | 0.47 | 0.0194 | 0.1155 | |
| 150 | 105.0 | 120 | 0.0245 | 0.32 | 0.74 | 0.02035 | unresolved | |

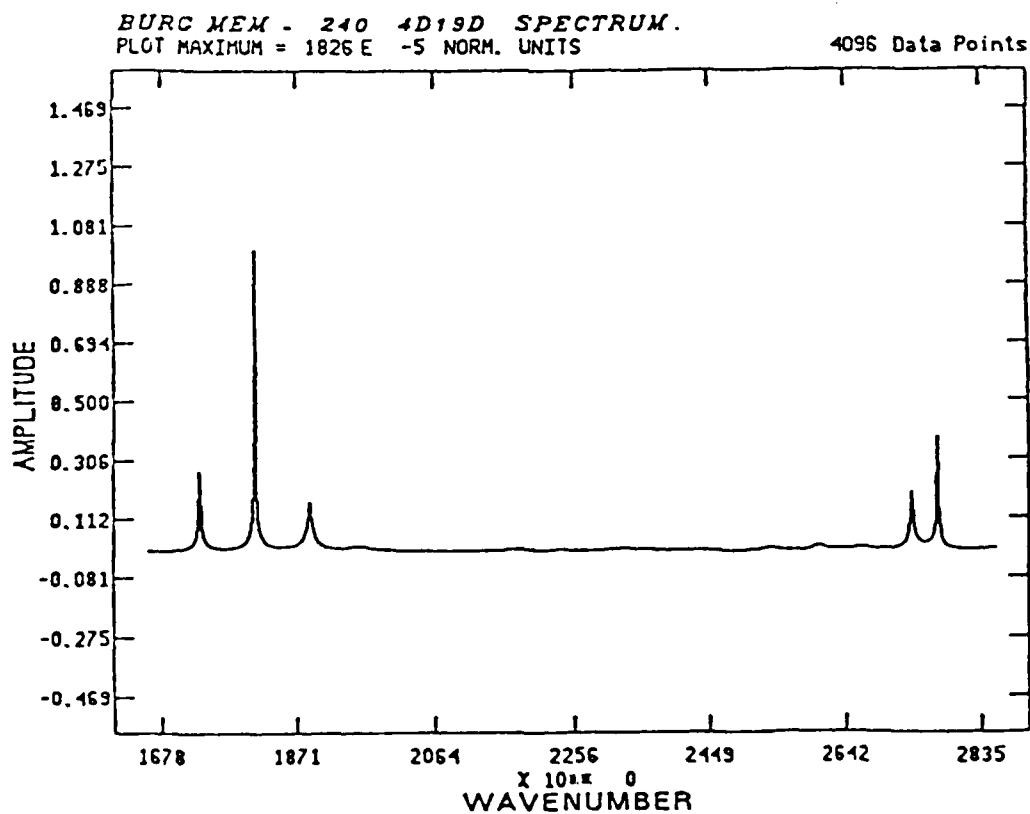


Figure 21. 600 Points of LABCEDE Interferogram Recovered with MEM.

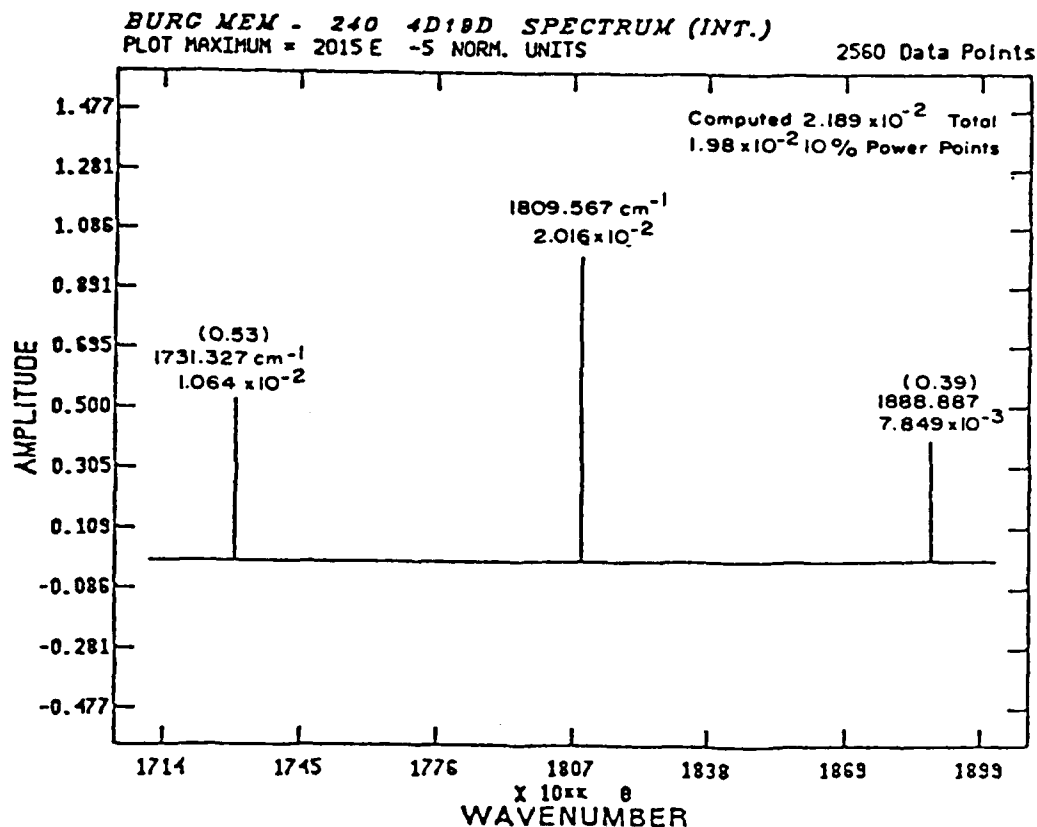


Figure 22. 600 Points of LABCEDE Interferogram Recovered with MEM and Integrated - Band 1.

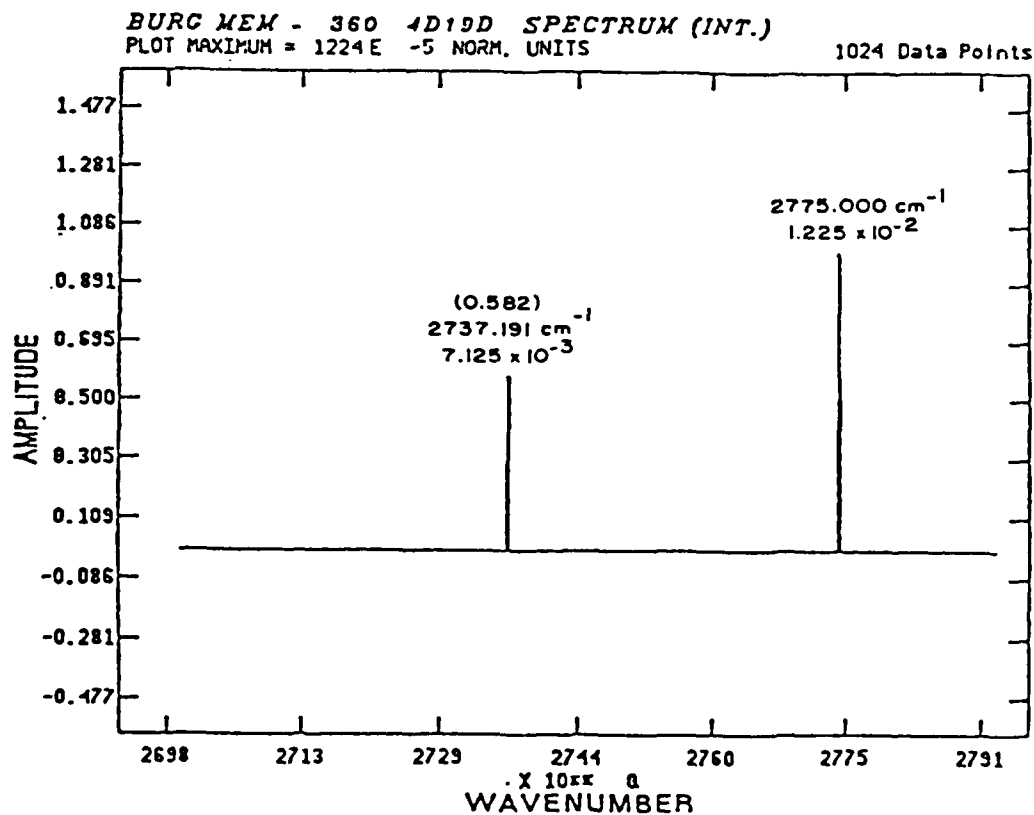


Figure 23. 600 Points of LABCEDE Interferogram Recovered with MEM and Integrated - Band 2.

3.3 Y-W MEM RESULTS

The Y-W MEM algorithm was then used to process the '4d19d' interferogram using the same procedure as the previous section. Basically the same results as the Burg MEM were obtained, i.e., a factor of two improvement over the conventional FFT algorithm.

Figure 25 is a spectrum of the 600 point interferogram recovered with 240 coefficients using the Y-W algorithm. One should compare this with Figure 21 recovered with the Burg algorithm with the same number of interferogram points and the same number of coefficients. A slightly better resolution was obtained with the Burg as concluded earlier. Table 3 lists the results of the Y-W MEM algorithm.

TABLE 3 Summary of Y-W Results
(Square-root PSD(f_o)df)

| # IF Points | 1st Zero Crossing (cm^{-1}) | # Coef. | Line Area | Norm. Line Area | | Area | Norm. Area |
|-------------|--|---------|---------------------------|---------------------------|---------|---------------------------|------------|
| | | | 1809 (cm^{-1}) | 1727 (cm^{-1}) | 1890 | 2778 (cm^{-1}) | 2738 |
| 1000 | 15.8 | 600 | | | | 0.01314 | 0.629 |
| | | 600 | | | | 0.01238 | 0.674 |
| 800 | 20.0 | 320 | 0.02084 | 0.491 | 0.371 | 0.00978* | 0.607* |
| | | 480 | | | | 0.01061** | 0.521** |
| 600 | 26.0 | 240 | 0.01957* | 0.511* | 0.401* | Barely Resolved | |
| 500 | 31.6 | 250 | 0.02148* | 0.496* | 0.422* | " | " |
| 400 | 40.0 | 240 | 0.02079* | 0.466* | 0.427* | " | " |
| | | | 0.0188** | 0.43** | 0.399** | " | " |

* Integrated between 20% power points

** Integrated between 50% power points

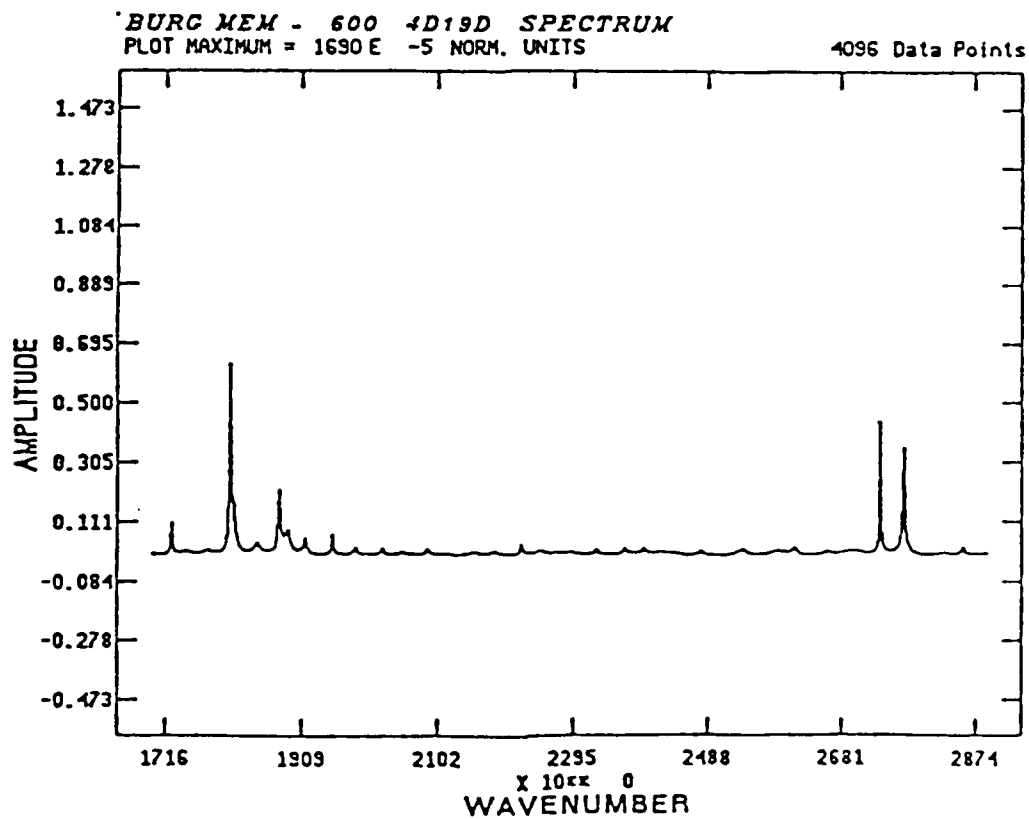


Figure 24. 1000 Points of LABCEDE Interferogram Recovered with MEM.

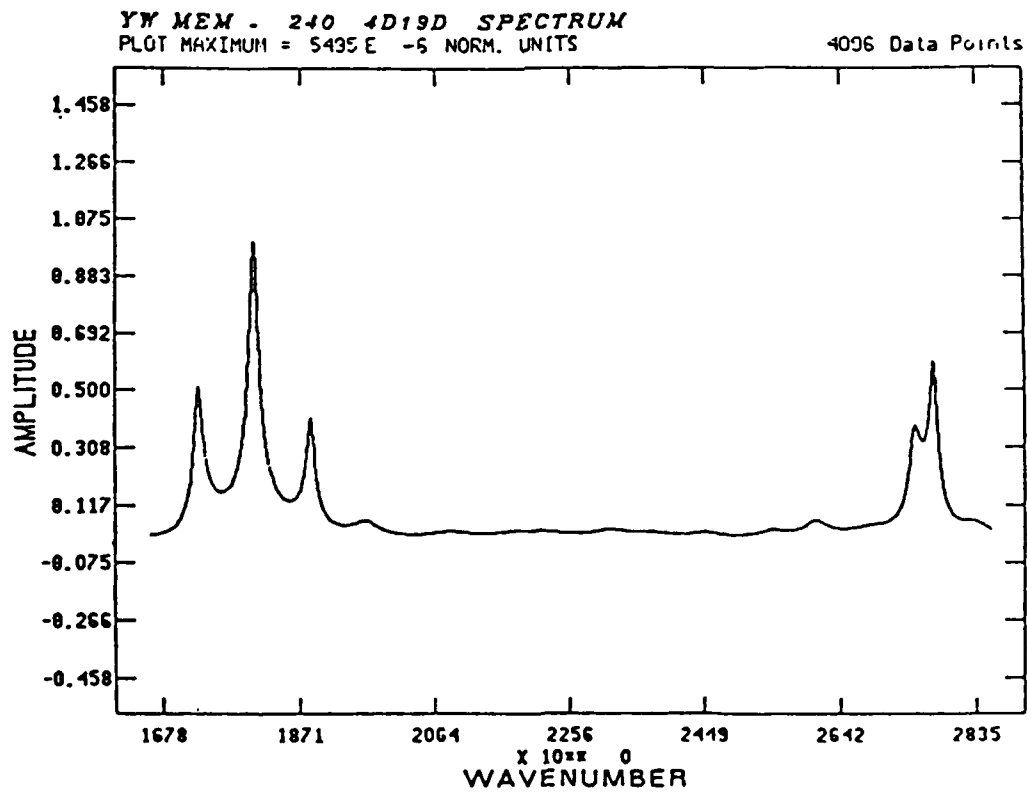


Figure 25. 600 Points of LABCEDE Interferogram Recovered with Y-W MEM.

This page intentionally left blank.

4.0 SUMMARY AND CONCLUSIONS

A systematic tradeoff was conducted on the FFT, Burg MEM, and the Y-W MEM algorithms in recovering spectral line data. The study was first conducted on synthetic data comprising of a cosine interferogram of spectral lines plus pseudo-random Gaussian white noise. Single and multiple spectra lines were used. The tradeoff was then performed on LABCEDE laboratory-measured data.

The following summarizes the results:

- (a) The Burg and Y-W MEM indicated a factor of two improvement over the FFT algorithm.
- (b) The PSD line profile obtained with the MEM was Lorentzian.
- (c) The MEM PSD line profile appeared independent of SNR.
- (d) The MEM PSD line width was linearly inversely proportional to the SNR for low SNRs.
- (e) The MEM PSD line width was linearly inversely proportional to the number of coefficients for small number of coefficients.
- (f) The linear relationship did not necessarily hold for multiple lines.
- (g) There was a line location error when the interferogram did not contain an integer number of quarter cycles of the waveform of a single line or two-line 'beat' frequency.
- (h) Individual line powers and power ratios were preserved when the lines were distinctly resolved.
- (i) Powers are preserved even when line power ratios were not.

- (j) An additional step was required for the MEM algorithms to compute the coefficients. The computational time required may be prohibitive for near real time applications.
- (k) A further search routine was necessary to locate the PSD line peaks and then to perform the area integration.

In summary, the pros and cons of the MEM technique in spectral recovery must be weighed for each application. It perhaps boils down to a tradeoff between data measurement time versus spectral recovery computational time. The choice therefore must be weighed for each application.

REFERENCES

1. Ulrych, T. J., Bishop, T. N., Maximum Entropy Spectral Analysis and Autoregressive Decomposition, Reviews of Geophysics and Space Physics, Vol. 13, No. 1, February 1975.
2. Radoski, H. R., Fougere, P. F., Zawalick, E. J., A comparison of Power Spectral Estimations and Applications of the Maximum Entropy Method, Journal of Geophysical Research, Vol. 80, No. 4, February 1975.
3. Anderson, N., On the Calculation of Filter Coefficients for Maximum Entropy Spectral Analysis, Geophysics, Vol. 39, No. 1, February 1974.
4. Kay, S. M., Marple, S. L. Jr., Spectrum Analysis - A Modern Perspective, Proceedings of the IEEE, Vol. 69, No. 11, November 1981.
5. Chen, W. Y., Stegen, G. R., Experiments with Maximum Entropy Power Spectra of Sinusoids, Journal of Geophysical Research, Vol. 79, No. 20, July 1974.

END

8-87

DTIC